ADAM10 mediates shedding of carbonic anhydrase IX ectodomain non-redundantly to ADAM17

MIRIAM ZATOVICOVA*, IVANA KAJANOVA*, MARTINA TAKACOVA, LENKA JELENSKA, OLGA SEDLAKOVA, MARTINA LABUDOVA and SILVIA PASTOREKOVA

Biomedical Research Center of the Slovak Academy of Sciences, Institute of Virology, Department of Tumor Biology, 84505 Bratislava, Slovakia

Received August 8, 2022; Accepted October 31, 2022

DOI: 10.3892/or.2022.8464

Abstract. Carbonic anhydrase IX (CA IX) is a transmembrane enzyme participating in adaptive responses of tumors to hypoxia and acidosis. CA IX regulates pH, facilitates metabolic reprogramming, and supports migration, invasion and metastasis of cancer cells. Extracellular domain (ECD) of CA IX can be shed to medium and body fluids by a disintegrin and metalloproteinase (ADAM) 17. Here we show for the first time that CA IX ECD shedding can be also executed by ADAM10, a close relative of ADAM17, via an overlapping cleavage site in the stalk region of CA IX connecting its exofacial catalytic site with the transmembrane region. This finding is supported by biochemical evidence using recombinant human ADAM10 protein, colocalization of ADAM10 with CA IX, ectopic expression of a dominant-negative mutant of ADAM10 and RNA interference-mediated suppression of ADAM10. Induction of the CA IX ECD cleavage with ADAM17 and/or ADAM10 activators revealed their additive effect. Similarly, additive effect was observed with an ADAM17-inhibiting antibody and an ADAM10-preferential inhibitor GI254023X. These data indicated that ADAM10 is a CA IX sheddase acting on CA IX non-redundantly to ADAM17.

Correspondence to: Professor Silvia Pastorekova, Biomedical Research Center of The Slovak Academy of Sciences, Institute of Virology, Department of Tumor Biology, Dubravska cesta 9, 84505 Bratislava, Slovakia
E-mail: silvia.pastorekova@savba.sk

*Contributed equally

Abbreviations: ADAM, a disintegrin and metalloproteinase; CA IX, carbonic anhydrase IX; CHO, Chinese hamster ovary cells; ECD, ectodomain; FL, full-length; GI, GI254023X; HIF, hypoxia-inducible factor; Mab, monoclonal antibody; ΔMP, dominant-negative mutant of ADAM10; NS, non-shed; PLA, proximity ligation assay; PMA, phorbol 12-myristate 13-acetate; TF, transcription factor; TIMP, tissue inhibitor of metalloproteinases

Key words: ADAM10, ADAM17, carbonic anhydrase IX, ectodomain shedding, internalization, cancer

Introduction

Ectodomain (ECD) shedding is an important regulatory mechanism, which controls spectrum and abundance of cell surface proteins mediating cellular responses to molecular and physiological signals (1). Concurrently, it generates soluble protein variants executing autocrine and/or paracrine signaling. Proper ECD shedding is essential for diverse biological processes, including cell fate decisions, proliferation, migration, metabolism, tissue and organ development, and its dysregulation contributes to various pathologies including cancer (2).

ECD shedding occurs via proteolytic cleavage of the extracellular portions of type I or II transmembrane proteins, or GPI-anchored proteins. It can be accomplished by various proteinases, among which a disintegrin and metalloproteinase (ADAM) family members have a prominent position (3,4). Out of 22 ADAM family members, ADAM17 and ADAM10 attract a lot of attention due to their functional implications in key signaling pathways. ADAM17, originally identified as TNFα-converting enzyme (TACE), is primarily related to EGFR signaling and represents a major sheddase for proinflammatory cytokines, whereas ADAM10 has been implicated mainly in Notch1 signaling and cleaves mostly cell adhesion molecules (5). However, ADAM17 and ADAM10 can also share several substrates (such as CD44, APP, DLL1, Notch, HB-EGF and TNFβ) suggesting that their complementary and/or compensatory activities are needed in certain cell or tissue contexts (6,7).

It was previously demonstrated by the authors that ADAM17 cleaves the ECD of carbonic anhydrase IX (CA IX) (8-11). CA IX is a cancer-associated, hypoxia-induced type I transmembrane protein participating in pH regulation, metabolic adaptation to hypoxia/acidosis and in cell migration-invasion-metastasis (12-17). CA IX ECD consists of two structural components: a highly active enzyme domain (CA) catalyzing the reversible conversion of carbon dioxide to bicarbonate and proton, and an N-terminal proteoglycan-like region (PG). While the CA domain catalytic activity participates in the control of tumor pH (14,15,18,19), the PG region mediates non-catalytic proton extrusion across the plasma membrane and is implicated in cell adhesion (20-24). A short stalk connecting the CA IX ECD to a single-pass transmembrane

region contains the ADAM17 cleavage site. Deletion of 10 amino acids from the stalk completely prevents CA IX ECD shedding and reinforces the tumorigenic phenotype of CA IX-expressing cells (11).

However, neither silencing nor inhibition of ADAM17 are sufficient to fully block CA IX ECD release suggesting that an additional protease can participate in this process (8,11). As ADAM10 is structurally and functionally related to ADAM17, its possible involvement in CA IX ECD shedding was investigated. In the present study, the first experimental evidence was provided using biochemical and molecular/cell biology approaches that ADAM10 can cleave the CA IX ECD via an overlapping cleavage site with ADAM17 and it was showed that both proteinases contribute to CA IX ECD shedding in a non-redundant manner.

Materials and methods

Cell culture. Wild-type hamster ovary CHOwt cells and human cervical carcinoma C33a cells were transfected with the full-length (FL) human CA9 cDNA and its non-shed (NS) deletion mutant (del393-402 aa) using TurboFect™ transfection reagent (Thermo Fisher Scientific, Inc.) as previously described (11). The cells were routinely cultured in DMEM medium with 10% FCS (BioWhittaker; Lonza Group, Ltd.) in a humidified atmosphere of 5% CO_2 at 37˚C. Cell lines have been authenticated using STR profiling within the past 3 years. All experiments were performed with mycoplasma-free cells.

rhADAM10 cleavage activity assays. Catalytic activity of recombinant rhADAM10 encompassing the catalytic domain (100 ng/ml, R&D Systems, Inc.) was verified by hydrolytic processing of Fluorogenic Peptide Substrate IX Mca-K-P-L-G-L-Dpa-A-R-NH_2 (10 μM; R&D Systems, Inc.) followed by monitoring of increasing fluorescence intensity at excitation and emission wavelengths of 320 and 405 nm (top read), respectively, in kinetic mode for 30, 40, 50 and 120 min at 37˚C using a Synergy H4 plate reader (BioTek Instruments, Inc.). All reactions were performed in a fluorogenic buffer containing 25 mM Tris pH 9, 150 mM NaCl, 2.5 μM $ZnCl_2$ and 0.005% Brij-35.

For the evaluation of ADAM10 cleavage of the cell membrane-bound CA IX, CHOwt cells transiently transfected with the FL human CA9 cDNA (CHOwt-FL-CA IX) and its deletion mutant NS CA IX (del393-402) (CHOwt-NS-CA IX), respectively, were treated with rhADAM10 (500 ng/ml) added to culture medium for 24 h. Thereafter, cell culture medium was harvested and CA IX ECD level was determined by ELISA.

Enzyme-linked immunosorbent assay (ELISA). For the CA IX ECD quantification, $1x10^5$ cells per well were seeded and cultured in a 24-well plate for 24 h. After medium exchange, the cells were incubated with either inhibitors or activators of shedding (as described below) and all supernatants were subsequently analyzed using in-house developed sandwich ELISA as previously described (8). The capture monoclonal antibody (Mab) V/10 specific for the catalytic domain of CA IX [10 μg/ml, generated in-house, (25)] was immobilized on the surface of microplate wells overnight at room temperature. After blocking and washing, diluted samples were added to the coated wells at room temperature for 2 h. The attached CA IX ECD was then allowed to react with the mixture of the PG domain-specific biotinylated Mabs [M75 and IV/18, generated and biotinylated in-house, (25)] diluted 1:7,500 (200 ng/ml) in the blocking buffer. The amount of bound detector antibodies was determined with peroxidase-conjugated streptavidin (Pierce; Thermo Fisher Scientific, Inc.) using the peroxidase substrate orthophenylene diamine (MilliporeSigma) after incubation for 1 h.

Indirect immunofluorescence. For detection of ADAM10, cells cultured on glass coverslips were incubated with anti-human ADAM10 ECD mouse Mab IgG2B Clone 163003 (R&D Systems, Inc.; cat. no. MAB1427, 1:100 in cultivation medium) for 1 h at 37˚C, gently washed with PBS and fixed with methanol for 5 min at -20˚C. Non-specific binding was blocked by incubation with PBS containing 1% BSA (MilliporeSigma) for 30 min at 37˚C. Cells were then incubated with secondary donkey anti-mouse IgG Alexa Fluor®488-conjugated antibody (Invitrogen; Thermo Fisher Scientific, Inc.; cat. no. A-21202) diluted 1:1,000 in the blocking buffer for 1 h at 37˚C. Finally, the coverslips were mounted onto slides in the Mounting Media with DAPI (cat. no. ab104139; Abcam), and analyzed by the confocal laser scanning microscope Zeiss LSM 510 Meta.

Proximity ligation assay (PLA). PLA was performed in a humid chamber at 37˚C according to the manufacturer's instructions (Olink) (26). Cells were seeded on glass coverslips and allowed to attach for 24 h. Then they were fixed with methanol, blocked with blocking buffer for 30 min and incubated with a mixture of antibodies against the ECDs of human CA IX (Abcam; rabbit, cat. no. ab15086) and ADAM10 (R&D Systems, Inc.; mouse MAB1427) each in 10 μg/ml concentration for 1 h. Following the incubation with plus and minus PLA probes for 1 h, a ligation mixture containing connector oligonucleotides and an amplification mixture containing fluorescently labeled DNA probe was added for 40 and 100 min, respectively. Samples were analyzed using a Zeiss LSM 510 Meta confocal microscope.

Internalization analyses. C33a-FL-CA IX (300,000 cells/dish) were plated on glass coverslips placed in Petri dishes of 3.5 cm diameter 24 h before the experiment. To analyze ADAM10 internalization induced by its inhibition, live cells were pre-incubated with anti-ADAM10 mouse MAB1427 from R&D Systems, Inc. (diluted 1:100 in culture medium) at 4˚C for 30 min. Then the culture medium was removed, replenished by the medium containing preferential ADAM10 inhibitor GI254023X (GI; 10 μM; MilliporeSigma) in DMSO at 0.1 % (v/v) final concentration and the cells were incubated for additional 2, 4, 8 or 24 h at 37˚C. Control samples were incubated without GI in medium containing DMSO at 0.1% (v/v) final concentration. After each incubation time point, parallel GI-treated and control samples were fixed for 5 min in ice-cold methanol at -20˚C and stored for subsequent immunofluorescence. All samples were then subjected to indirect immunofluorescence using secondary donkey anti-mouse Alexa Fluor®488-conjugated antibody (Invitrogen; Thermo Fisher Scientific, Inc.; cat. no. A-21202) diluted 1:1,000 in

blocking buffer containing 1% BSA for 1 h at 37˚C. Finally, the coverslips were mounted onto slides in the Mounting Media with DAPI, and analyzed by a confocal laser scanning microscope Zeiss LSM 510 Meta.

To analyze the ADAM10 subcellular localization in response to internalization of CA IX, live cells were pre-incubated with anti-ADAM10 mouse MAB1427 from R&D Systems, Inc. (diluted 1:100 in culture medium) simultaneously with anti-CA IX humanized CA9hu-1 Mab capable of stimulating CA IX internalization [50 μg/ml; provided by Professor J. Pastorek, MABPRO, a.s. (27)] at 4˚C for 30 min. Control samples were pre-incubated with anti-ADAM10 mouse MAB1427 only. Immediately after removal from 4˚C, samples were transferred to 37˚C to allow for internalization and then incubated for additional 2, 4, 8 and 24 h. After each incubation time point, parallel samples were fixed with methanol and stored as aforementioned. Fixed and blocked control samples that were not pre-treated with the CA9hu-1 antibody at the beginning of the experiment were post-incubated with that antibody, for 1 h at 37˚C. All samples were then incubated with the mixture of secondary donkey anti-mouse Alexa Fluor®488-conjugated antibodies and goat anti-human Alexa Fluor®555-conjugated antibodies (Invitrogen; Thermo Fisher Scientific, Inc.; cat. no. A-21433) diluted 1:1,000 in the blocking buffer containing 1% BSA for 1 h at 37˚C. Finally, the coverslips were mounted onto slides in Mounting Media with DAPI, and analyzed by the confocal laser scanning microscope Zeiss LSM 510 Meta.

Reverse transcription-quantitative PCR (RT-qPCR). Total RNA was isolated using RNeasy Plus Mini Kit (Qiagen) and reverse transcription of 1 μg RNA for each sample was performed with the High-Capacity cDNA Reverse Transcription kit (Applied Biosystems; Thermo Fisher Scientific, Inc.) according to the manufacturer's instructions. qPCR was carried out using Maxima SYBR Green PCR Master mix (Thermo Fisher Scientific, Inc.) with the following gene-specific primers: ADAM10 sense, 5'-GACCACAGA CTTCTCCGGAAT-3' and antisense 5'-TGAAGGTGCTCC AACCCAAG-3'; ADAM17 sense, 5'-TGGATGAAGGAG AAGAGTGTGA-3' and antisense, 5'-AAGATCCAAGCA AACAGTGTCAT-3'; and β-actin sense, 5'-TCCTCCCTG GAGAAGAGCTA-3' and antisense, 5'-ACATCTGCTGGA AGGTGGAC-3'. qPCR was performed for 10 min at 95˚C for initial denaturation followed by 40 cycles of 95˚C for 15 sec and 60˚C for 1 min. Sample CT values were normalized to β-actin. Relative expression was calculated using the $2^{-\Delta\Delta Cq}$ method (28). All amplifications were performed in triplicates.

RNA interference. For siRNA-mediated silencing of *de novo* ADAM10 synthesis, C33a-FL-CA IX cells were seeded at $8x10^4$ cells/cm^2. One day later, cells were transfected with 1 μg of either MISSION® enzymatically-prepared small interfering RNA (esiRNA) human ADAM10 (Sigma-Aldrich; Merck KGaA; cat. no. EHU129311) or control esiRNA targeting RLUC (Sigma-Aldrich; Merck KGaA; cat. no. EHURLUC) using Attractene transfection reagent (Qiagen) according to the manufacturer's recommendations. Briefly, esiRNA was diluted in serum-free DMEM medium and Attractane Transfection Reagent in a total volume of 100 μl, and incubated for 15 min at room temperature. Following the medium exchange, the transfection reagent/esiRNA mixture was added drop-wise onto C33a-FL-CA IX cells. The day after transfection, cells were incubated with fresh cultivation medium either with or without 10 μM GI inhibitor for 24 h [as previously described (29)] and subsequently processed for ELISA analysis. Effect of ADAM10 silencing was evaluated by RT-qPCR in transfected versus control cells.

Expression of dominant-negative mutant of ADAM10 (ΔMP). C33a-FL-CA IX cells were plated into 35-mm Petri dishes to reach ~70% monolayer density on the next day. Transient transfection was performed with 6 μg of pcDNA3-Delta (Pro-MP) ADAM10-HA plasmid encoding a ΔMP mutant lacking prodomain and metalloprotease domain, a gift from Axel Ullrich (Addgene, Inc; plasmid cat. no. 65107; http://n2t.net/addgene:65107; RRID: Addgene_65107) using TurboFect™ reagent according to the manufacturer's recommendation. Briefly, plasmid DNA (6 μg) was diluted in serum-free DMEM medium and TurboFect Transfection Reagent in a total volume of 200 μl, and incubated for 15 min at room temperature. The transfection reagent/plasmid DNA mixture was added drop-wise to each dish without medium exchange. Cells transfected with empty vector served as negative control. One day later, transfected cells were trypsinized and plated in six-well plates. Half of the transfected cells were incubated in the presence of GI inhibitor diluted in DMEM to working concentration of 10 μM. As a negative control, DMSO was added in a volume corresponding to the concentration of the inhibitor. After 24 h, proteins from transfected cells were extracted and cell culture medium was collected for ELISA.

Western blotting. Western blotting was performed as previously described (8). In brief, C33a-FL-CA IX and C33a-NS-CA IX cells were lysed in ice-cold RIPA buffer (150 mM NaCl, 1% Triton X-100, 0.05% NaDOC, 1 mM EDTA, 0.1% SDS, 50 mM Tris-HCl pH 7.4) containing inhibitors of proteases (Roche Applied Science). Cell lysates were collected and cleared by centrifugation at 10,000 x g for 15 min at 4˚C. Total protein concentration was determined using the BCA protein assay reagent (Thermo Fisher Scientific, Inc.) and 50 μg/ml of total proteins mixed with Laemmli buffer were loaded per lane, separated in 10% SDS-PAGE and transferred onto PVDF membrane (Macherey-Nagel GmbH; cat. no. 741260). The membranes were treated with blocking buffer containing 5% (w/v) non-fat milk with 0.2% Nonidet P40 for 1 h and probed with the following primary antibodies: in-house generated anti-CA IX M75 Mab (hybridoma medium 1:3 in 5% non-fat dry milk with 0.2% Nonidet P40 in PBS, 1 h, room temperature); anti-ADAM17 (cat. no. 3976; 1:1,000 in 3% BSA in TBS-T buffer, overnight, 4˚C), anti-ADAM10 (cat. no. 14194; 1:1,000 in 3 % BSA in TBS-T buffer, overnight, 4˚C); anti-β-actin (cat. no. 3700) 1:5,000 in 3% BSA in TBS-T buffer (0,1% Tween-20), 1 h, room temperature; all from Cell Signaling Technology, Inc). After washing with 0.1% Tween-20 in PBS, the membranes were incubated for 1 h at room temperature, with the secondary antibodies: HRP-conjugated goat anti-mouse IgG (Sigma-Aldrich; Merck KGaA; cat. no. A0168) or HRP-conjugated goat anti-rabbit IgG (Bio-Rad Laboratories, Inc.; cat. no. 1721019) diluted

1:5,000 in blocking buffer for 1 h at room temperature. Protein bands were detected using enhanced chemiluminescence kit (GE Healthcare Bio-Sciences).

Activation and inhibition of CA IX ECD shedding. For the activation of shedding, treatment of cells with phorbol-12-myristate-13-acetate (PMA; MilliporeSigma) at 20 μM final concentrations, and/or ionomycin (IONO; MilliporeSigma) at final concentration of 1 μg/ml was performed for 3 h. For the inhibition of shedding, cells were treated with serum-free medium containing preferential ADAM10 inhibitor GI (1 μM), and/or ADAM17-inhbiting antibody D1(A12) (200 nM; Abcam; cat. no. ab215268) for 3 h at 37˚C.

Bioinformatics. *In silico* analysis of the ADAM10 and ADAM17 promoters was performed using MatInspector (https://www.genomatix.de) (30,31). The promoter sequences with the overall length of 1,418 and 1,643 bp were extracted directly from the ElDorado genome database for the ADAM10 and ADAM17 genes, respectively. Transcription factors (TFs) were selected according to the core (0.75) and matrix (optimized) similarity. The accurate position of predicted binding elements was calculated according to the transcription start site. Phenotype heatmaps containing comparisons of relative transcriptional patterns of CA9, ADAM10, and ADAM17 in tumor tissue specimens from glioblastoma and colorectal carcinoma patients were generated through IST (in silico transcriptomics) online Medisapiens database (https://ist.medisapiens.com, accessed on March 10, 2021, currently available at https://tracxn.com/d/companies/medisapiens.com).

Statistical analysis. Data were analyzed using unpaired two-tailed Student's t-test or one-way ANOVA with Dunnett's multiple comparison test using GraphPad Prism 9 (GraphPad Software, Inc.). P<0.05 was considered to indicate a statistically significant difference.

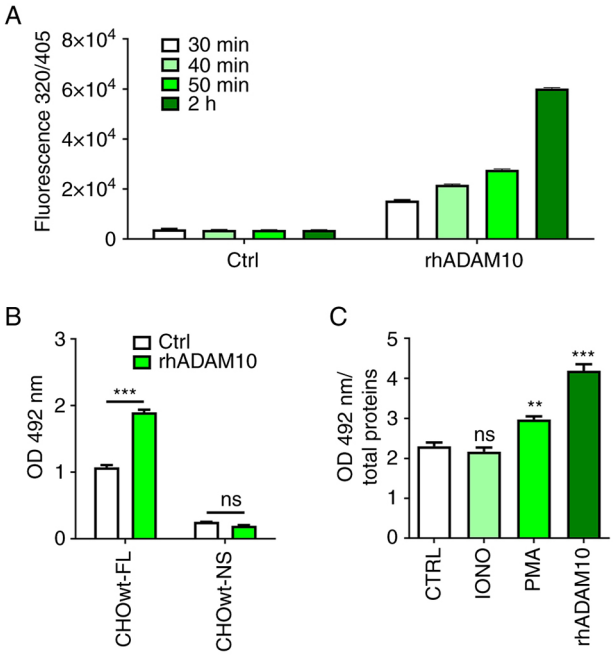

Figure 1. Biochemical evidence for ADAM10-mediated CA IX ECD cleavage. (A) Verification of the cleavage activity of rhADAM10 catalytic domain towards the fluorogenic peptide Mca-K-P-L-G-L-Dpa-A-R-NH_2. The peptide was used at the final concentration of 10 μM in a total of 100 μl reaction mixture with 10 ng of the rhADAM10. The cleavage was allowed to proceed for 30, 40, 50 and 120 min. Time-related increase of the fluorescence emitted from the peptide proves that rhADAM10 was active in comparison to negative control without rhADAM10. (B) ELISA analysis of CA IX ECD in culture medium obtained from CHOwt-FL-CA IX and CHOwt-NS-CA IX cells transiently expressing FL-CA IX and NS-CA IX, respectively. Transfected cells were treated with rhADAM10 (500 ng/ml) for 24 h (Data were analyzed by Student's t-test). (C) Incubation of CHOwt-FL-CA IX cells with ADAM17 activator PMA (20 μM, 3 h), ADAM10 activator IONO (1 μg/ml, 3 h) or rhADAM10 (500 ng/ml, 24 h). Data were analyzed using one-way ANOVA followed by Dunnett's test. Experiments were performed in triplicates and repeated twice. The results were expressed as the mean ± SD. **P<0.01 and ***P<0.001. ADAM, a disintegrin and metalloproteinase; CA IX, carbonic anhydrase IX; rhADAM10, recombinant human ADAM10; ECD, ectodomain; FL, full-length; NS, non-shed; IONO, ionomycin; PMA, phorbol 12-myristate 13-acetate; ns, non-significant.

Results

CA IX cleavage by recombinant human ADAM10. It was first aimed to gain biochemical evidence that CA IX is an ADAM10 substrate. Therefore, a recombinant human ADAM10 catalytic domain (rhADAM10) was used, the activity of which was proven by the cleavage of a commercial fluorogenic peptide (Fig. 1A). RhADAM10 was then shown to cleave a transiently expressed full-length (FL) CA IX from the surface of transfected wild-type CHOwt cells, that express a functional ADAM17 proteinase, but lack an endogenous ADAM10 proteinase (Fig. 1B). In line with this finding, incubation of CHOwt-FL-CA IX cells with ADAM17 activator PMA resulted in shedding of CA IX ECD, while ADAM10 activator IONO had no effect (Fig. 1C). However, CA IX ECD was shed to culture medium upon external addition of rhADAM10 (Fig. 1C).

Moreover, rhADAM10 was used to treat transiently transfected CHOwt-NS-CA IX cells expressing the NS CA IX variant generated by the deletion of 10 amino acids from the stalk region (11). As recently demonstrated, the NS CA IX variant exhibits cell surface expression similar to FL CA IX (11). Even though rhADAM10 was able to significantly increase the level of ECD shed from FL CA IX, it could not cleave the NS CA IX variant (Fig. 1B). These findings demonstrated that CA IX is a direct ADAM10 substrate and that the ADAM10 cleavage site is localized in the fragment deleted from the NS variant, which also contains the cleavage site for ADAM17 (11).

Colocalization and proximity of ADAM10 and CA IX. The role of endogenous ADAM10 in ECD shedding from the CA IX protein expressed on the surface of human cancer cells was next examined. For this purpose, stably transfected C33a cervical carcinoma cells constitutively expressing FL CA IX were employed. C33a-FL-CA IX cells express ADAM10 at the mRNA and protein levels and subcellular localization similar to control C33a-neo cells, as demonstrated by indirect immunofluorescence using the MAB1427 antibody specific for human ADAM10 (Fig. 2A and B). To further explore the spatial relationship between ADAM10 and CA IX, PLA was performed, which visualizes protein-protein interactions

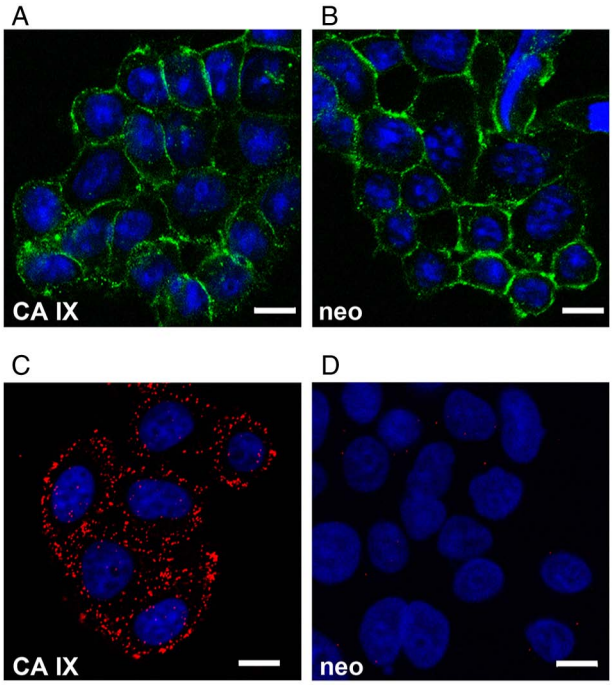

Figure 2. Co-localization of ADAM10 and CA IX in C33a-FL-CA IX cells. Immunofluorescence of (A) C33a-FL-CA IX cells expressing CA IX, and (B) control C33a-neo cells using ADAM10-specific antibody. Nuclei were counterstained with DAPI. PLA performed in (C) C33a-FL-CA IX and (D) C33a-neo cells using rabbit anti-human CA IX-specific antibody and mouse anti-human ADAM10 antibody. Red PLA signal indicating the interaction of CA IX with ADAM10 was clearly visible only in C33a cells expressing FL CA IX. Experiment was performed in triplicates and repeated twice. Magnification, x630. Scale bar, 10 μm. ADAM, a disintegrin and metalloproteinase; CA IX, carbonic anhydrase IX; PLA, proximity ligation assay; FL, full-length.

in situ. This in-cell co-immunoprecipitation represents an alternative to conventional co-immunoprecipitation of extracted proteins while preserving the natural context of the analyzed interactors (26). PLA was executed with the primary antibodies binding to the N-terminal regions of ADAM10 and CA IX. Results revealed a clear fluorescent signal suggesting that ADAM10 is in close proximity and can interact with CA IX (Fig. 2C). No PLA signal was observed in the control C33a-neo cells (Fig. 2D).

Co-internalization of ADAM10 and CA IX. It was next aimed to determine whether ADAM10 remains co-distributed with CA IX during internalization induced by the specific CA9hu-1 Mab directed to the CA IX catalytic domain (27). For that purpose, C33a-FL-CA IX cells were first incubated at 4˚C with both anti-ADAM10 and anti-CA IX antibodies to enable their binding only to the subpopulation of ADAM10 and CA IX molecules present on the cell surface. Control samples were pre-treated only with ADAM10 antibody, which is unable to trigger internalization. The pre-bound antibodies could enter the cells together with their antigens only via active endocytosis (i.e. internalization), which was facilitated by transferring the cells to 37˚C. This approach allowed us to observe the endocytosis and recycling of the complexes of the primary antibodies bound to their antigens throughout the experimental period and detect them with the corresponding secondary antibodies at different time points. In the absence of internalization-inducing CA9hu-1 antibody, both CA IX and ADAM10 displayed plasma membrane localization (Fig. 3A-D). By contrast, CA9hu-1 antibody-induced internalization of CA IX was clearly visible already after 2 h and was accompanied by internalization of ADAM10 as indicated by their overlapping fluorescence signals (Fig. 3E-G). Later on, both molecules recycled back to the plasma membrane (Fig. 3G and H).

Effect of molecular targeting of ADAM10 on CA IX ECD shedding. Based on the aforementioned observations, it was aimed to directly target ADAM10 expression in C33a-FL-CA IX cells by RNA interference and follow its impact on CA IX ECD shedding. The initial attempts to suppress ADAM10 were not fully satisfactory despite the clear downregulation of ADAM10 transcription (Fig. S1A), possibly due to the fact that the reduced *de novo* synthesis of ADAM10 protein remained unrecognized within the large pool of existing ADAM10 molecules. To solve this problem, an approach inspired by the study of Seifert *et al* (29) was chosen, where it was revealed that exposing cells to GI, a preferential ADAM10 inhibitor that binds to the protease active-site, leads to its internalization followed by lysosomal degradation of mature ADAM10 molecules. Therefore, it was assumed that inactivation linked to a reduction in the pool of existing mature ADAM10 molecules would enhance the effect of ADAM10 suppression. We first verified that GI causes the ADAM10 internalization also in C33a-FL-CA IX cells (Fig. 4). This was performed by pre-incubation of live cells with anti-ADAM10 antibody to allow for its binding only to the molecules exposed on the cell surface. Then the cells were incubated with or without GI at 37˚C to enable endocytosis. Afterwards, the cells were fixed and stained with the secondary antibody. The cells without added GI inhibitor displayed ADAM10 on the plasma membrane (Fig. 4A-D). By contrast, exposure of cells to 10 μM GI at 37˚C led to a reduced membrane localization of ADAM10 apparently due to its internalization (Fig. 4E-H).

Then, transient esiRNA-mediated ADAM10 silencing was performed, followed by 24 h incubation of the transfected cells with and without GI inhibitor at 10 μM concentration (Fig. 4I). Rather than using a single chemically-synthesized siRNA, it was decided to employ an esiRNA made up of a diverse pool of siRNA that all target the same mRNA sequence. Each individual siRNA has a lower concentration in the pool, leading to lower off-target effects while producing an efficient knockdown. Alternatively, transient expression of a ΔMP lacking the pro- and metalloprotease domains was accomplished (Figs. 4J and S1B) (32) again followed by the 24 h treatment with or without 10 μM GI. As recently demonstrated, the long-term effect (24 h) of 10 μM GI is limited to ADAM10 and not observed for ADAM17, which is not a primary target of this inhibitor (29). Culture media from cells subjected to esiRNA or ΔMP transfections incubated with and without GI were then analyzed for CA IX ECD by ELISA (Fig. 4I and J).

Both approaches led to similar effects on CA IX ECD shedding (Fig. 4I and J). Targeting of ADAM10 alone reduced CA IX ECD release to medium by 9% for esiRNA and 18% for ΔMP. Silencing of *de novo* synthesis was inferior compared with the ΔMP expression as ΔMP protein could potentially

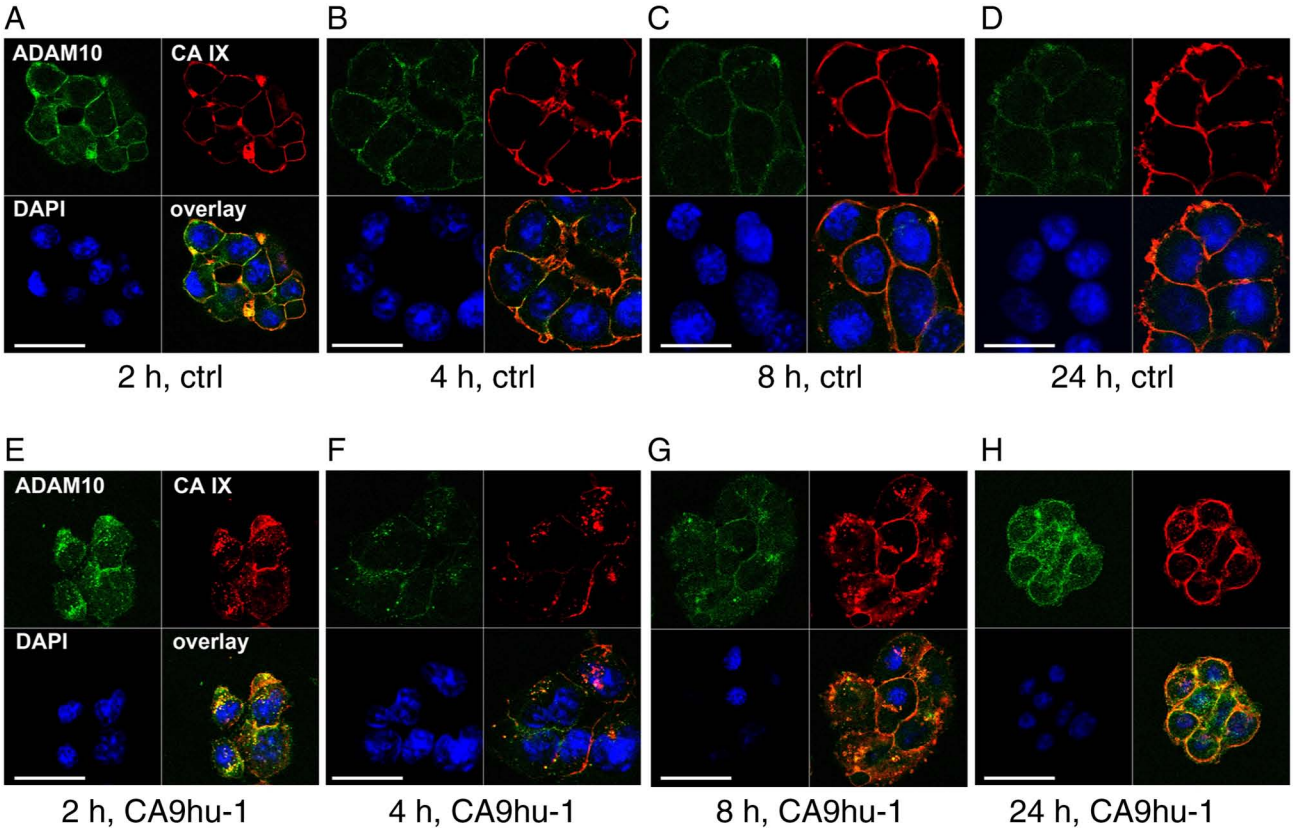

Figure 3. Localization of ADAM10 (green) in response to CA9hu-1 antibody-induced CA IX internalization (red). C33a-FL-CA IX cells were pre-incubated either with anti-ADAM10 antibody alone (ctrl, A-D) or with anti-ADAM10 antibody together with the internalization-inducing anti-CA IX antibody CA9hu-1 (E-H) 30 min at 4˚C. Plasma membrane staining signal for ADAM10 and CA IX was observed at all time points in the absence of CA9hu-1 pre-treatment. On the other hand, CA9hu-1-induced internalization of CA IX as well as ADAM10 was visible after 2 and 4 h at 37˚C (E and F), while both molecules showed recycling to plasma membrane after 8 and 24 h. Overlapped staining signals were evident in all samples. Magnification, x630. Scale bar, 20 μm. Experiment was performed in triplicates and repeated twice. ADAM, a disintegrin and metalloproteinase; CA IX, carbonic anhydrase IX.

dimerize with existing ADAM10 molecules and perturb their function. Inhibition of mature ADAM10 by GI in non-transfected cells decreased CA IX ECD shedding by 15% for esiRNA and 28% for ΔMP. However, simultaneous targeting and inhibition of ADAM10 resulted in 37% (esiRNA) and 41% (ΔMP) reduction of CA IX ECD release to the culture medium. These data are in line with the aforementioned biochemical and co-localization experiments and further support the view that ADAM10 is involved in the CA IX ECD shedding.

Additive effects of ADAM10 and ADAM17 activators and inhibitors on CA IX ECD shedding. Since C33a cells express both ADAM10 (Fig. 2A) and ADAM17 (11), they represent a suitable cell model to investigate possible relationship between these two ADAMs in CA IX ECD shedding. qPCR analysis of C33a cells revealed that the level of ADAM10 transcript is significantly higher (~2.5-times) than the level of ADAM17 in these cells irrespectively of whether they express FL CA IX or NS CA IX (Fig. 5A). Expression of both metalloproteinases in C33a cells was also revealed by Western blotting (Fig. 5B). Although the intensity of protein bands appeared to be similar, these two results cannot be directly compared due to the fact that the antibodies specific for ADAM10 and ADAM17, respectively, may differ in the binding properties. As revealed in the present study for ADAM10 (Figs. 2 and 3) and recently for ADAM17 (11) by indirect immunofluorescence of live cells, both metalloproteinases are localized on the cell surface in CA IX proximity where they can accomplish CA IX ECD cleavage.

C33a-FL-CA IX cells were treated either with IONO that is known to activate primarily ADAM10 or with PMA predominantly activates ADAM17 (33), or simultaneously with both activators to find out their individual and combined effect on activated CA IX ECD shedding. Medium was harvested from the cells treated with activators for 3 h and analyzed for CA IX ECD by ELISA. As revealed in Fig. 5C, each activator was able to significantly increase the level of CA IX ECD from C33a-FL-CA IX cells and moreover, they showed an additive effect when used together. No basal ECD shedding and no activation was observed in C33a-NS-CA IX cells (data not shown).

C33a-FL-CA IX cells were then treated with inhibitors (Fig. 5D), namely the ADAM17-inhibiting antibody D1(A12) that binds to a conformation-sensitive cross-domain epitope on ADAM17 molecule (34) and GI at 1 μM concentration that is fully specific for ADAM10 and not sufficient for inhibition of ADAM17 in this experimental setting (35) (Fig. S1D). D1(A12) Mab was used because it is specific only for ADAM17, whereas other known ADAM10 inhibitor, a hydroxamate-based TAPI-0, can inhibit not only ADAM17 but also MMP metalloproteinases and potentially also carbonic anhydrases (36). GI was used at 1 μM concentration, since at 10 μM concentration it could slightly reduce shedding of CA IX from the surface of

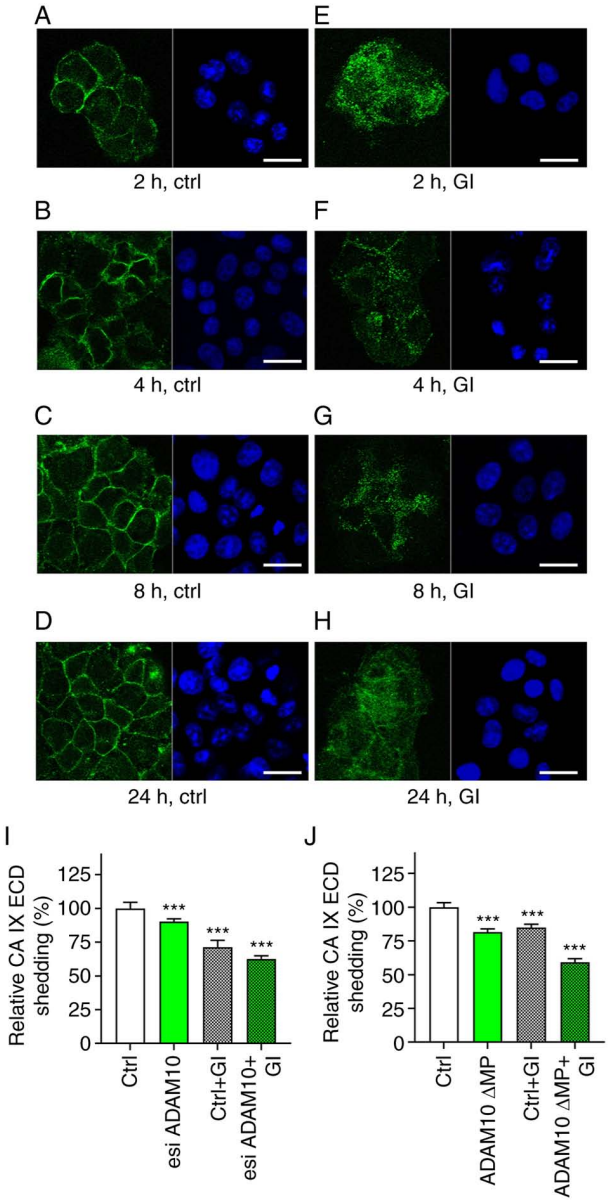

Figure 4. GI-induced internalization of ADAM10 and targeting of ADAM10 by RNA interference or by a dominant-negative ADAM10 mutant ΔMP. (A-H) C33a-FL-CA IX cells were pre-incubated with anti-ADAM10 antibody at 4˚C. (A-D) Cells showed the plasma membrane staining signal for ADAM10 (green) in absence of GI at 37˚C. (E-H) GI-induced internalization of ADAM10 was clearly visible as cytoplasmic staining signal in all incubation periods at 37˚C. (I) Direct targeting of ADAM10 was performed by RNA interference and (J) expression of a dominant-negative mutant ΔMP with and without GI treatment. Control cells were transfected with either an esiRNA targeting RLUC or an empty vector (pcDNA3.1). Culture media collected from transfected cells incubated in presence and absence of GI for 24 h were collected and subjected to ELISA analysis for detection of CA IX ECD. Experiment was performed in triplicates and repeated six times. Data were analyzed by one-way ANOVA followed by Dunnett's test. Results were expressed as the mean percentage of CA IX ECD shedding with control cells set as 100% ± SD. ***P<0.001. GI, GI254023X; ADAM, a disintegrin and metalloproteinase; ΔMP, dominant-negative mutant of ADAM10; esiRNA, enzymatically-prepared small interfering RNA; CA IX, carbonic anhydrase IX; ECD, ectodomain.

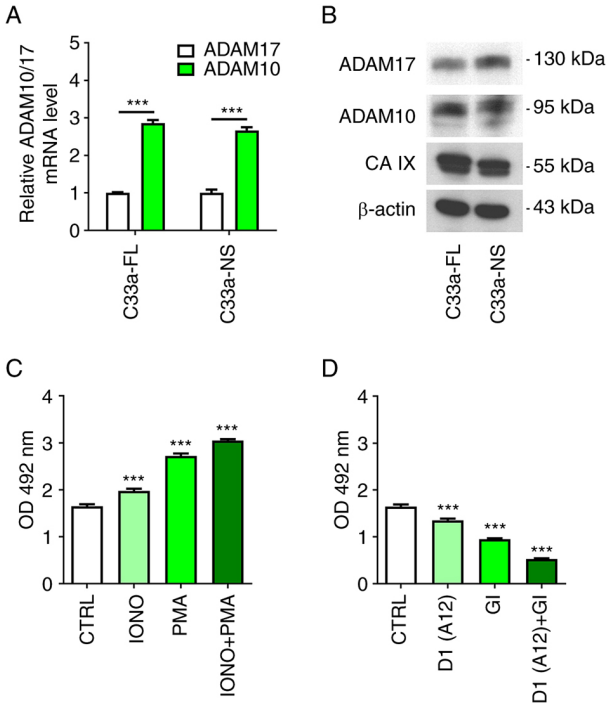

Figure 5. Additive effect of ADAM10 and ADAM17 activation/inhibition. (A) Quantitative PCR analysis of ADAM10 and ADAM17 mRNA levels in C33a-FL-CA IX and C33a-NS-CA IX cells normalized to the level of β-actin mRNA. (B) Western blot analysis of ADAM10, ADAM17 and CA IX protein in C33a-FL-CA IX and C33a-NS-CA IX cells. The anti-actin antibody was used as a loading control. (C and D) ELISA analysis of CA IX ECD in culture medium collected from C33-FL-CA IX cells after the treatment with IONO (1 μg/ml), PMA (20 μM), IONO + PMA (1 μg/ml; 20 μM), D1(A12) antibody (200 nM), GI inhibitor (1 μM) or D1(A12) + GI (200 nM; 1 μM) for 3 h in comparison to non-treated cells (CTRL). Experiment was performed in triplicates and repeated two times. Data were analyzed by (A) Student's t-test and (C and D) one-way ANOVA followed by Dunnett's test. Results were expressed as the mean relative levels of mRNA or CA IX ECD ± SD. ***P<0.001. ADAM, a disintegrin and metalloproteinase; FL, full-length; CA IX, carbonic anhydrase IX; NS, non-shed; ECT, ectodomain; IONO, ionomycin; PMA, phorbol 12-myristate 13-acetate; GI, GI254023X.

live CHO cells that express only ADAM17 but not ADAM10 (Fig. S1C and D). In the internalization experiments, slight inhibition of ADAM17 alongside full inhibition of ADAM10 did not interfere with the ADAM10 endocytosis. However, in the experiments aimed at CA IX ECD shedding from C33a cells that express both sheddases, it was required to be certain that GI specifically inhibits only ADAM10. Importantly, a significant additive effect of inhibitors was observed on constitutive CA IX shedding from C33a-FL-CA IX (Fig. 5D), suggesting contribution of both ADAM17 and ADAM10.

Collectively, these data suggested that CA IX ECD shedding is mediated not only by ADAM17, as previously described (8,11), but also by ADAM10, as demonstrated in the present study.

Discussion

CA IX is a cancer-associated carbonic anhydrase isoform expressed in a broad range of tumor types, where it is primarily localized on the surface of cells exposed to chronic hypoxia and/or cells with oncogenic mutation(s) leading to activation of the hypoxia-inducible factor (HIF) pathway. The cell surface position allows CA IX to use the exofacial catalytic domain to regulate tumor pH via reversible conversion of CO_2 generated by oncogenic metabolism to bicarbonate ions and protons. Bicarbonate ions are imported into the cytoplasm by

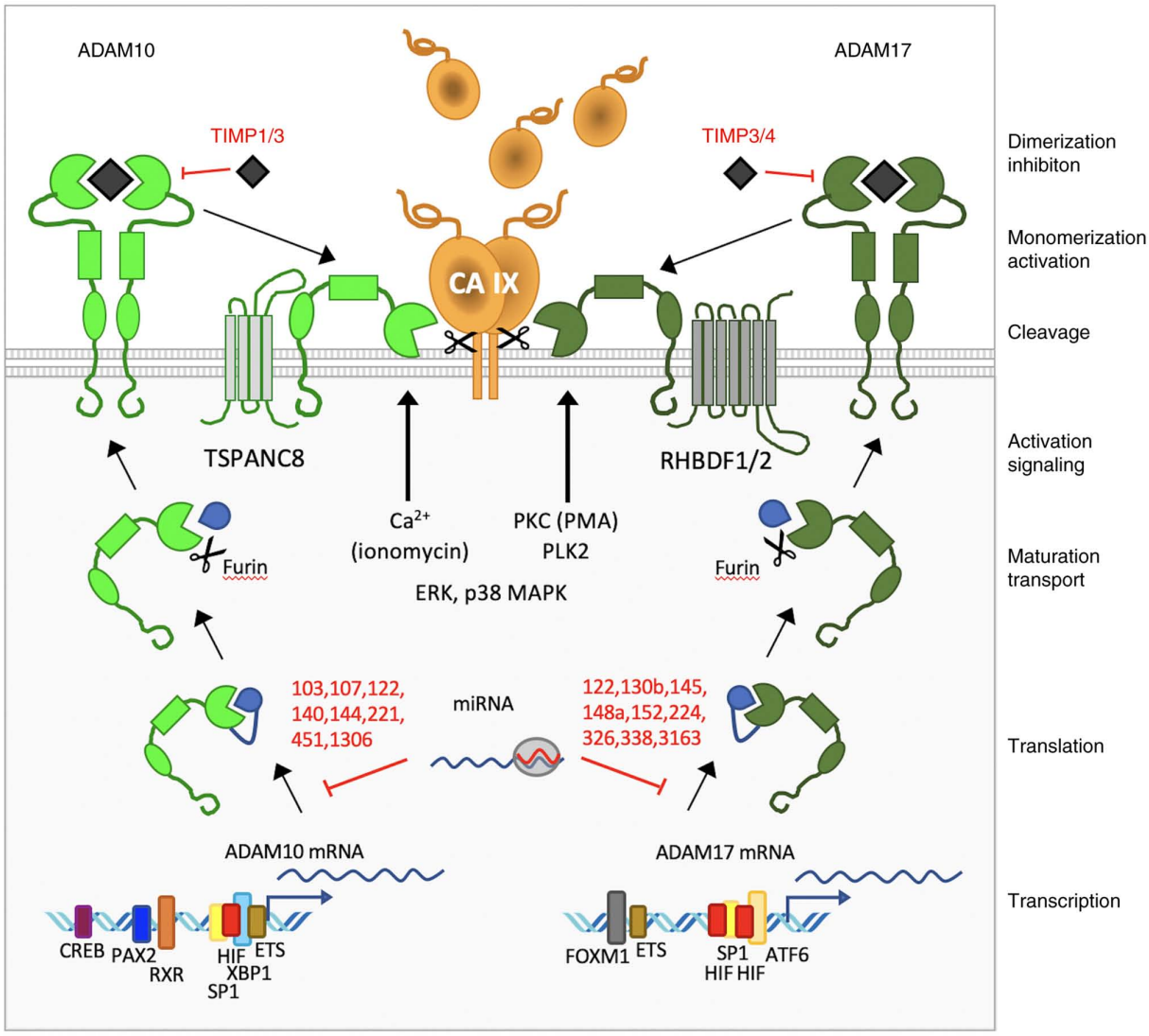

Figure 6. Scheme illustrating CA IX ECD shedding by ADAM10 and ADAM17 proteinases. Picture depicts differences in regulatory components that differentially affect ADAMs biosynthesis and processing at various levels of their expression and activation and thereby can potentially influence CA IX ECD cleavage. Based on (33,40-51). CA IX, carbonic anhydrase IX; ADAM, a disintegrin and metalloproteinase; ECD, ectodomain.

bicarbonate transporters to maintain slightly alkaline intracellular pH, which is crucial for cell survival and proliferation, whereas protons remain in pericellular space and contribute to extracellular acidosis, which supports invasiveness and metastasis. The N-terminal proteoglycan-like region of the extracellular domain of CA IX mediates cell adhesion and participates in a non-catalytic export of protons in co-operation with lactate transporters [reviewed in (13,37)].

It was previously demonstrated by the authors that CA IX is a highly stable protein with a half-life close to 40 h (38). However, ~10% of the CA IX molecules undergo constitutive shedding of their ECD, which is sensitive to metalloproteinase inhibitor batimastat (8). Even though hypoxia increases the level of the shed ECD, the fraction of the soluble CA IX ECD is proportional to the hypoxia-induced expression of the cell-associated protein. Nevertheless, it was identified that CA IX ECD shedding can be increased by PMA, which activates ADAM17 through the PKC pathway, and both biochemical and molecular evidences were provided for the ADAM17-mediated CA IX shedding via the cleavage site localized in the stalk region proximal to the transmembrane region of the CA IX molecule (8,11).

In the present study, it was shown for the first time that CA IX ECD can be also cleaved by ADAM10. In addition, it was demonstrated that CA IX and ADAM10 are localized in close proximity. This is further supported by the finding that the antibody-triggered internalization of CA IX is associated with the internalization of ADAM10. Both molecules exhibit overlapping subcellular distribution not only during endocytosis, but also during recycling to the plasma membrane indicating that they remain associated throughout the intracellular path. Thus, the co-localization of ADAM10 with CA IX fulfils the spatial prerequisite for their interaction and CA IX ECD cleavage.

The data obtained with the NS CA IX variant suggested that ADAM10 can mediate CA IX ECD shedding via the cleavage site overlapping with that of ADAM17. Based on comparison of the sequence of amino acids deleted from the NS mutant with the predicted cleavage sites for dual ADAM10&17 substrates (39), it can be deduced that the

cleavage site may be localized on the CA IX molecule between the positions 402*403 corresponding to PRAAE*PVQ sequence. Moreover, data obtained in the present study supported the view that ADAM10 and ADAM17 proteinases are involved in both constitutive shedding (as demonstrated by inhibitors) and activated shedding (as demonstrated by activators) of CA IX.

ADAM10 is regulated by different pathways and can cleave a spectrum of molecular targets only partially overlapping with targets of ADAM17 (5,33). Thus, ADAM10 appears to facilitate CA IX ECD shedding in additional signaling and physiological contexts, and thereby can affect responses mediated by soluble CA IX also in the absence of ADAM17. Based on previous data by the authors, soluble CA IX appears to interfere with the local functions of the cell-tethered CA IX protein that are required for tumorigenic and metastatic phenotype, including proper execution of the pH-regulatory and adhesion functions, presumably via competitive interactions with CA IX partner proteins in the plasma membrane or in the extracellular space (11).

When looking more closely at the regulation and effector functions of ADAM10 versus ADAM17, a large diversity of molecular events can be observed, that play a role in distinct expression patterns as well as activities of these two related proteinases, which execute CA IX ECD shedding (Fig. 6).

Data from the literature and from *in silico* analysis of ADAM10 and ADAM17 promoters using the MatInspector tool (Fig. S2) suggested involvement of the general TF SP1 through multiple binding sites in transcription of both ADAM10 and ADAM17 genes (40,41). Both genes were also shown to be transcriptionally activated by hypoxia (42,43). Typical hypoxia-response element sequences recognized by the HIF TF were found and functionally proven in ADAM17 promoter, while ADAM10 promoter appears to contain just a HIF-ancillary sequence and two ARNT (i.e. HIF-β) binding sequences. In addition, both ADAM10 and ADAM17 promoters include several binding sites for ETS1 factor, which can cooperate with other TFs, including CREB, SP1 and HIF. Notably, while ADAM10 seems to respond also to moderate hypoxia (0.5-5% of oxygen), ADAM17 is transcriptionally induced by severe hypoxia (below 0.1% O_2) (42,43). Moreover, transcription of ADAM10 was shown to be induced by retinoic acid (RA) through its binding to RA receptor and retinoid receptors to RXR motifs in the ADAM10 promoter (40). ADAM10 (but not ADAM17) is also regulated by paired box 2 TF, particularly in WT1-mutated kidney cancers through multiple promoter binding sites and by XBP1 factor involved in response to DNA damage (44-46). On the other hand, ADAM17 transcription is regulated by forkhead box M1 (47). Both ADAM10 and ADAM17 can be also regulated post-transcriptionally by distinct sets of miRNAs (48).

Another level of expression diversity is given by the post-translational regulation. Maturation of ADAM10 depends on tetraspanins (TSPANC8), whereas maturation of ADAM17 is driven by rhomboid chaperones iRhom1 and iRhom2 encoded by RHBDF1 and 2 genes (49,50). Moreover, ADAM10 can be inhibited by tissue inhibitor of metalloproteinase (TIMP) 1 and TIMP3, whereas ADAM17 can be inhibited by the TIMP3 and TIMP4 molecules, which are expressed in various tumor types at various levels and can locally impair the cleavage of ADAMs' substrates including CA IX (51). Finally, activation of shedding can be mediated either by release of Ca^{2+} ions through ADAM10 or by pathways involving PKC, EGFR/PI3K, ERK, TNFα or NF-κB signaling through ADAM17 (33).

All these circumstances create specific tumor tissue contexts, where the shedding of CA IX ECD may depend on multiple factors such as those driving the expression of CA IX, expression of ADAM10 and ADAM17, or on their inhibitors and activators (Fig. 6). This complex picture is evident from the phenotype heatmap generated by IST Medisapiens (https://ist.medisapiens.com) analysis of the RNA-seq metadata for glioblastoma and colorectal carcinoma, illustrating expression of selected genes in tumor tissues of individual patients (Fig. S3A and B). The analysis showed distinct transcription patterns of CA IX, ADAM17 and ADAM10, suggesting that in certain CA IX-expressing tumors lacking ADAM17, CA IX ECD shedding can be potentially executed by ADAM10. This renders CA IX shedding possible in a broader range of tumor tissues. Similarly, distinct expression patterns can be observed also in other tumor types.

Accumulating experimental and clinical studies demonstrate correlations of CA IX expression in cancer or stromal cells to aggressive tumor phenotype, poor patient prognosis and resistance to therapy. However, potential clinical value of CA IX ECD shedding remains unclear despite numerous efforts to exploit soluble CA IX as non-invasive tumor biomarker. While certain studies support its prognostic and/or predictive value, others do not show any significant relationship between the CA IX ECD levels and clinical parameters. This can be at least in part due to complex regulation of the CA IX ECD shedding. Uncovering the involvement of ADAM10 in the CA IX ECD cleavage sheds a new light on this intricate phenomenon and represents an important step towards its improved understanding in terms of both tumor biology and clinical applications.

Acknowledgements

The authors would like to thank professor Jaromír Pastorek (MABPRO, a. s.) for generous gift of the CA9hu-1 Mab and Dr Tereza Golias (Biomedical Research Center SAS) for language editing.

Funding

The present study was supported by the Slovak Scientific Grant Agency (grant nos. VEGA 2/0074/20 and VEGA 2/0076/20), the Research & Developmental Support Agency (grant nos. APVV-15-0697 and APVV-19-0098) and the George Schwab and Leona Lauder Foundation.

Availability of data and materials

All data generated or analyzed during this study are included in this published article.

Authors' contributions

MZ, IK and MT designed and performed the experiments, analyzed/interpreted the data and contributed to the

manuscript writing. LJ contributed to immunofluorescence and ELISA assays. OS performed the qPCR experiments. ML contributed to confocal microscopy. MT performed bioinformatic analyses. SP designed the study, supervised the experiments, interpreted the data, wrote and edited the manuscript. MZ, IK and MT confirm the authenticity of all raw data. All authors have read and approved the final version of the manuscript.

Ethics approval and consent to participate

Not applicable.

Patient consent for publication

Not applicable.

Competing interests

SP, MZ and MT are co-inventors of patents related to CA IX. The remaining authors declare that they have no competing interests.

References

1. Lichtenthaler SF, Lemberg MK and Fluhrer R: Proteolytic ectodomain shedding of membrane proteins in mammals-hardware, concepts, and recent developments. EMBO J 37: e99456, 2018.
2. Hayashida K, Bartlett AH, Chen Y and Park PW: Molecular and cellular mechanisms of ectodomain shedding. Anat Rec (Hoboken) 293: 925-937, 2010.
3. Murphy G: The ADAMs: Signalling scissors in the tumour microenvironment. Nat Rev Cancer 8: 929-941, 2008.
4. Mullooly M, McGowan PM, Crown J and Duffy MJ: The ADAMs family of proteases as targets for the treatment of cancer. Cancer Biol Ther 17: 870-880, 2016.
5. Saftig P and Reiss K: The 'A Disintegrin And Metalloproteases' ADAM10 and ADAM17: Novel drug targets with therapeutic potential? Eur J Cell Biol 90: 527-535, 2011.
6. Pruessmeyer J and Ludwig A: The good, the bad and the ugly substrates for ADAM10 and ADAM17 in brain pathology, inflammation and cancer. Semin Cell Dev Biol 20: 164-174, 2009.
7. Vincent B and Checler F: α-Secretase in Alzheimer's disease and beyond: Mechanistic, regulation and function in the shedding of membrane proteins. Curr Alzheimer Res 9: 140-156, 2012.
8. Zaťovičová M, Sedláková O, Švastová E, Ohradanova A, Ciampor F, Arribas J, Pastorek J and Pastorekova S: Ectodomain shedding of the hypoxia-induced carbonic anhydrase IX is a metalloprotease-dependent process regulated by TACE/ADAM17. Br J Cancer 93: 1267-1276, 2005.
9. Zaťovičová M and Pastoreková S: Modulation of cell surface density of carbonic anhydrase IX by shedding of the ectodomain and endocytosis. Acta Virol 57: 257-264, 2013.
10. Vidlickova I, Dequiedt F, Jelenska L, Sedlakova O, Pastorek M, Stuchlik S, Pastorek J, Zatovicova M and Pastorekova S: Apoptosis-induced ectodomain shedding of hypoxia-regulated carbonic anhydrase IX from tumor cells: A double-edged response to chemotherapy. BMC Cancer 16: 239, 2016.
11. Kajanova I, Zatovicova M, Jelenska L, Sedlakova O, Barathova M, Csaderova L, Debreova M, Lukacikova L, Grossmannova K, Labudova M, *et al*: Impairment of carbonic anhydrase IX ectodomain cleavage reinforces tumorigenic and metastatic phenotype of cancer cells. Br J Cancer 122: 1590-1603, 2020.
12. Russell S, Xu L, Kam Y, Abrahams D, Ordway B, Lopez AS, Bui MM, Johnson J, Epstein T, Ruiz E, *et al*: Proton export upregulates aerobic glycolysis. BMC Biol 20: 163, 2022.
13. Pastorek J and Pastoreková S: Hypoxia-induced carbonic anhydrase IX as a target for cancer therapy: From biology to clinical use. Semin Cancer Biol 31: 52-64, 2015.
14. Švastová E, Hulíková A, Rafajová M, Zat'ovicová M, Gibadulinová A, Casini A, Cecchi A, Scozzafava A, Supuran CT, Pastorek J and Pastoreková S: Hypoxia activates the capacity of tumor-associated carbonic anhydrase IX to acidify extracellular pH. FEBS Lett 577: 439-445, 2004.
15. Švastová E, Witarski W, Csaderová L, Kosik I, Skvarkova L, Hulikova A, Zatovicova M, Barathova M, Kopacek J, Pastorek J and Pastorekova S: Carbonic anhydrase IX interacts with bicarbonate transporters in lamellipodia and increases cell migration via its catalytic domain. J Biol Chem 287: 3392-3402, 2012.
16. Benej M, Svastova E, Banova R, Kopacek J, Gibadulinova A, Kery M, Arena S, Scaloni A, Vitale M, Zambrano N, *et al*: CA IX stabilizes intracellular pH to maintain metabolic reprogramming and proliferation in hypoxia. Front Oncol 10: 1462, 2020.
17. Gibadulinova A, Bullova P, Strnad H, Pohlodek K, Jurkovicova D, Takacova M, Pastorekova S and Svastova E: CAIX-mediated control of LIN28/let-7 axis contributes to metabolic adaptation of breast cancer cells to hypoxia. Int J Mol Sci 21: 4299, 2020.
18. Swietach P, Patiar S, Supuran CT, Harris AL and Vaughan-Jones RD: The role of carbonic anhydrase 9 in regulating extracellular and intracellular pH in three-dimensional tumor cell growths. J Biol Chem 284: 20299-20310, 2009.
19. Chiche J, Ilc K, Laferriere J, Trottier E, Dayan F, Mazure NM, Brahimi-Horn MC and Pouysségur J: Hypoxia-inducible carbonic anhydrase IX and XII promote tumor cell growth by counteracting acidosis through the regulation of the intracellular pH. Cancer Res 69: 358-368, 2009.
20. Závada J, Závadová Z, Pastorek J, Biesová Z, Jezek J and Velek J: Human tumour-associated cell adhesion protein MN/CA IX: Identification of M75 epitope and of the region mediating cell adhesion. Br J Cancer 82: 1808-1813, 2000.
21. Jamali S, Klier M, Ames S, Barros LF, McKenna R, Deitmer JW and Becker HM: Hypoxia-induced carbonic anhydrase IX facilitates lactate flux in human breast cancer cells by non-catalytic function. Sci Rep 5: 13605, 2015.
22. Ames S, Pastorekova S and Becker HM: The proteoglycan-like domain of carbonic anhydrase IX mediates non-catalytic facilitation of lactate transport in cancer cells. Oncotarget 9: 27940-27957, 2018.
23. Csaderová L, Debreová M, Radvák P, Stano M, Vrestiakova M, Kopacek J, Pastorekova S and Svastova E: The effect of carbonic anhydrase IX on focal contacts during cell spreading and migration. Front Physiol 4: 1-12, 2013.
24. Radvák P, Repic M, Švastová E, Takacova M, Csaderova L, Strnad H, Pastorek J, Pastorekova S and Kopacek J: Suppression of carbonic anhydrase IX leads to aberrant focal adhesion and decreased invasion of tumor cells. Oncol Rep 29: 1147-1153, 2013.
25. Zaťovičová M, Tarábková K, Švastová E, Gibadulinová A, Mucha V, Jakubícková L, Biesová Z, Rafajová M, Gut MO, Parkkila S, *et al*: Monoclonal antibodies generated in carbonic anhydrase IX-deficient mice recognize different domains of tumour-associated hypoxia-induced carbonic anhydrase IX. J Immunol Methods 282: 117-134, 2003.
26. Söderberg O, Gullberg M, Jarvius M, Ridderstråle K, Leuchowius KH, Jarvius J, Wester K, Hydbring P, Bahram F, Larsson LG and Landegren U: Direct observation of individual endogenous protein complexes in situ by proximity ligation. Nat Methods 3: 995-1000, 2006.
27. Zatovicova M, Kajanova I, Barathova M, Takacova M, Labudova M, Csaderova L, Jelenska L, Svastova E, Pastorekova S, Harris AL and Pastorek J: Novel humanized monoclonal antibodies for targeting hypoxic human tumors via two distinct extracellular domains of carbonic anhydrase IX. Cancer Metab 10: 3, 2022.
28. Livak KJ and Schmittgen TD: Analysis of relative gene expression data using real-time quantitative PCR and the 2(-Delta Delta C(T)) method. Methods 25: 402-408, 2001.
29. Seifert A, Düsterhöft S, Wozniak J, Koo CZ, Tomlinson MG, Nuti E, Rossello A, Cuffaro D, Yildiz D and Ludwig A: The metalloproteinase ADAM10 requires its activity to sustain surface expression. Cell Mol Life Sci 78: 715-732, 2021.
30. Cartharius K, Frech K, Grote K, Klocke B, Haltmeier M, Klingenhoff A, Frisch M, Bayerlein M and Werner T: MatInspector and beyond: Promoter analysis based on transcription factor binding sites. Bioinformatics 21: 2933-2942, 2005.
31. Quandt K, Frech K, Karas H, Wingender E and Werner T: MatInd and matInspector: New fast and versatile tools for detection of consensus matches in nucleotide sequence data. Nucleic Acids Res 23: 4878-4884, 1995.

32. Gschwind A, Hart S, Fischer OM and Ullrich A: TACE cleavage of proamphiregulin regulates GPCR-induced proliferation and motility of cancer cells. EMBO J 22: 2411-2421, 2003.
33. Le Gall S, Bobé P, Reiss K, Horiuchi K, Niu XD, Lundell D, Gibb DR, Conrad D, Saftig P and Blobel CP: ADAMs 10 and 17 represent differentially regulated components of a general shedding machinery for membrane proteins such as transforming growth factor α, L-selectin, and tumor necrosis factor alpha. Mol Biol Cell 20: 1785-1794, 2009.
34. Tape CJ, Willems SH, Dombernowsky SL, Stanley PL, Fogarasi M, Ouwehand W, McCafferty J and Murphy G: Cross-domain inhibition of TACE ectodomain. Proc Natl Acad Sci U S A 108: 5578-5583, 2011.
35. Ludwig A, Hundhausen C, Lambert M, Broadway N, Andrews RC, Bickett DM, Leesnitzer MA and Becherer JD: Metalloproteinase inhibitors for the disintegrin-like metalloproteinases ADAM10 and ADAM17 that differentially block constitutive and phorbol ester-inducible shedding of cell surface molecules. Comb Chem High Throughput Screen 8: 161-171, 2005.
36. Supuran CT: How many carbonic anhydrase inhibition mechanisms exist? J Enzyme Inhib Med Chem 31: 345-360, 2016.
37. Becker HM: Carbonic anhydrase IX and acid transport in cancer. Br J Cancer 122: 157-167, 2020.
38. Rafajová M, Zatovicová M, Kettmann R, Pastorek J and Pastoreková S: Induction by hypoxia combined with low glucose or low bicarbonate and high posttranslational stability upon reoxygenation contribute to carbonic anhydrase IX expression in cancer cells. Int J Oncol 24: 995-1004, 2004.
39. Tucher J, Linke D, Koudelka T, Cassidy L, Tredup C, Wichert R, Pietrzik C, Becker-Pauly C and Tholey A: LC-MS based cleavage site profiling of the proteases ADAM10 and ADAM17 using proteome-derived peptide libraries. J Proteome Res 13: 2205-2214, 2014.
40. Prinzen C, Müller U, Enders K, Fahrenholz F and Postina R: Genomic structure and functional characterization of the human ADAM10 promoter. FASEB J 11: 1522-1524, 2005.
41. Szalad A, Katakowski M, Zheng X, Jiang F and Chopp M: Transcription factor Sp1 induces ADAM17 and contributes to tumor cell invasiveness under hypoxia. J Exp Clin Cancer Res 28: 129, 2009.
42. Barsoum IB, Hamilton TK, Li X, Cotechini T, Miles EA, Siemens DR and Graham CH: Hypoxia induces escape from innate immunity in cancer cells via increased expression of ADAM10: Role of nitric oxide. Cancer Res 71: 7433-7441, 2011.
43. Rzymski T, Petry A, Kračun D, Rieß F, Pike L, Harris AL and Görlach A: The unfolded protein response controls induction and activation of ADAM17/TACE by severe hypoxia and ER stress. Oncogene 31: 3621-3634, 2012.
44. Lee SB, Doberstein K, Baumgarten P, Wieland A, Ungerer C, Bürger C, Hardt K, Boehncke WH, Pfeilschifter J, Mihic-Probst D, *et al*: PAX2 regulates ADAM10 expression and mediates anchorage-independent cell growth of melanoma cells. PLoS One 6: e22312, 2011.
45. Doberstein K, Pfeilschifter J and Gutwein P: The transcription factor PAX2 regulates ADAM10 expression in renal cell carcinoma. Carcinogenesis 32: 1713-1723, 2011.
46. Reinhardt S, Schuck F, Grösgen S, Riemenschneider M, Hartmann T, Postina R, Grimm M and Endres K: Unfolded protein response signaling by transcription factor XBP-1 regulates ADAM10 and is affected in Alzheimer's disease. FASEB J 28: 978-997, 2014.
47. Kim IM, Ramakrishna S, Gusarova GA, Yoder HM, Costa RH and Kalinichenko VV: The Forkhead Box m1 transcription factor is essential for embryonic development of pulmonary vasculature. J Biol Chem 280: 22278-22286, 2005.
48. Vincent B: Regulation of the α-secretase ADAM10 at transcriptional, translational and post-translational levels. Brain Res Bull 126: 154-169, 2016.
49. Matthews AL, Noy PJ, Reyat JS and Tomlinson MG: Regulation of A disintegrin and metalloproteinase (ADAM) family sheddases ADAM10 and ADAM17: The emerging role of tetraspanins and rhomboids. Platelets 28: 333-341, 2017.
50. Düsterhöft S, Babendreyer A, Giese AA, Flasshove C and Ludwig A: Status update on iRhom and ADAM17: It's still complicated. Biochim Biophys Acta Mol Cell Res 1866: 1567-1583, 2019.
51. Jackson HW, Defamie V, Waterhouse P and Khokha R: TIMPs: Versatile extracellular regulators in cancer. Nat Rev Cancer 17: 38-53, 2017.